Anal. Chem. **2007,** *79,* 4442−4447

Biocompatible Conductive Architecture of Carbon Nanofiber-Doped Chitosan Prepared with Controllable Electrodeposition for Cytosensing

Chen Hao,[†] Lin Ding,[†] Xueji Zhang,[‡] and Huangxian Ju*,[†]

MOE Key Laboratory of Analytical Chemistry for Life Science, Department of Chemistry, Nanjing University, Nanjing 210093, People's Republic of China, and Department of Chemistry, University of South Florida, 4202 East Fowler Avenue, CHE 305, Tampa, Florida 33620-5250

A novel architecture was designed by combining the biocompatibility of chitosan (CS) and excellent conductivity of carbon nanofiber (CNF). The controllable electrodeposition of soluble CNF-doped CS colloidal solution formed a robust CNF−CS nanocomposite film with good biocompatibility for the immobilization and cytosensing of K562 cells on an electrode. The formed architecture was characterized using scanning electron microscopic, infrared spectrum, contact angle, and thermogravimetric analyses. The adhesion of K562 cells on the nanocomposite film-modified electrode could be followed with electrochemical impedance spectroscopy and cyclic voltammetry. The presence of CNF facilitated the electrochemical behavior of K562 cells. The impedance of electronic transduction was related to the amount of the adhered cells, producing a highly sensitive impedance sensor for K562 cells ranging from 5×10^3 to 5.0×10^7 cells mL^{-1} with a limit of detection of 1×10^3 cells mL^{-1}. This work suggested a strategy to prepare a biocompatible and conductive interface for immobilization and electrochemical detection of cells and opened a way for the application of CNF in cytosensing.

Carbon nanofiber (CNF), as one of the nanoscale carbonaceous materials, has recently attracted considerable attention owing to its unique mechanical, structural, and catalytic properties, excellent electrical conductivity and chemical stability, and tunable surface functionalities, resulting in a wide range of applications such as CNF-supported Ni, Pt, Co, and Ru catalysts,[1−4] fuel cells,[5] probe tips,[6] CNF−silica nanocomposite film,[7] templates for preparation of oxide nanotubes,[8] and chemical or biosensors.[9−13] Compared with carbon nanotubes (CNTs), an extensively applied nanoscale carbonaceous material, CNF has low production cost and easier mass production,[14] better mechanical stability,[6] and larger surface-active groups-to-volume ratio.[9] Particularly, CNF possesses more edge sites on the outer wall than CNTs,[15] which facilitate the electron transfer of electroactive analytes. Based on this advantage, a highly sensitive biosensor has been proposed for detection of both NADH and ethanol at a low overpotential as described in our previous work.[13] This work further designed a biocompatible CNF-based surface for immobilization of living cells by electrodeposition of soluble CNF-doped chitosan (CS) colloidal solution. Compared with the traditional techniques for film preparation, the electrodeposition method is simple, controllable, and reproducible.

CNF has been used as a novel electrical−neural interface material[16] for neuroelectroanalytical measurements of intercellular communication between excitable cells,[17] with which the quantal release of easily oxidized transmitters following direct culture and differentiation can be observed. The excellent conductivity of CNF is beneficial in the design of more effective neural prostheses,[18] providing the opportunities for fundamental neuroelectronics

* Corresponding author. Tel./Fax: +86-25-83593593. E-mail: hxju@nju.edu.cn.

[†] Nanjing University.

[‡] University of South Florida.

(1) van der Lee, M. K.; Jos van Dillen, A.; Bitter, J. H.; de Jong, K. P. *J. Am. Chem. Soc.* **2005**, *127*, 13573−13582.

(2) Zhang, L.; Cheng, B.; Samulski, E. T. *Chem. Phys. Lett.* **2004**, *398*, 505−510.

(3) Bezemer, G. L.; Falke, U.; van Dillen, A. J.; de Jong, K. P. *Chem. Commun.* **2005**, *6*, 731−733.

(4) Toebes, M. L.; Prinsloo, F. F.; Bitter, J. H.; Van Dillen, J. A.; De Jong, K. P. *J. Catal.* **2003**, *214*, 78−87.

(5) Hacker, V.; Wallnofer, E.; Baumgartner, W.; Schaffer, T.; Besenhard, J. O.; Schrottner, H.; Schmied, M. *Electrochem. Commun.* **2005**, *7*, 377−382.

(6) Cui, H.; Kalinin, S. V.; Yang, X.; Lowndes, D. H. *Nano Lett.* **2004**, *4*, 2157−2161.

(7) Niedziolka, J.; Murphy, M. A.; Marken, F.; Opallo, M. *Electrochim. Acta* **2006**, *51*, 5897−5903.

(8) Ogihara, H.; Sadakane, M.; Nodasaka, Y.; Ueda, W. *Chem. Mater.* **2006**, *18*, 4981−4983.

(9) Vamvakaki, V.; Tsagaraki, K.; Chaniotakis, N. *Anal. Chem.* **2006**, *78*, 5538−5542.

(10) Pruneanu, S.; Ali, Z.; Watson, G.; Hu, S. Q.; Lupu, D.; Biris, A. R.; Olenic, L.; Mihailescu, G. *Part. Sci. Technol.* **2006**, *24*, 311−320.

(11) Zhang, B.; Fu, R. W.; Zhang, M. Q.; Dong, X. M.; Wang, L. C.; Pittman, C. U. *Mater. Res. Bull.* **2006**, *41*, 553−562.

(12) Wei, G.; Fujiki, K.; Saitoh, H.; Shirai, K.; Tsubokawa, N. *Polym. J.* **2004**, *36*, 316−322.

(13) Wu, L. N.; Zhang, X. J.; Ju, H. X. *Anal. Chem.*, in press.

(14) Jang, J.; Bae, J.; Choi, M.; Yoon, S.-H. *Carbon* **2005**, *43*, 2730−2736.

(15) Kim, S.-U.; Lee, K.-H. *Chem. Phys. Lett.* **2004**, *400*, 253−257.

(16) Nguyen-Vu, T. D. B.; Chen, H.; Cassell, A. M.; Andrews, R.; Meyyappan, M.; Li, J. *Small* **2006**, *2*, 89−94.

(17) McKnight, T. E.; Melechko, A. V.; Fletcher, B. L.; Jones, S. W.; Hensley, D. K.; Peckys, D. B.; Griffin, G. D.; Simpson, M. L.; Ericson, M. N. *J. Phys. Chem. B* **2006**, *110*, 15317−15327.

(18) McKenzie, J. L.; Waid, M. C.; Shi, R. Y.; Webster, T. J. *Biomaterials* **2004**, *25*, 1309−1317.

10.1021/ac062344z CCC: $37.00
Published on Web 05/11/2007

research.[16] Although this material has been used for selective bone cells adhesion due to its good mechanical properties,[19] and nanometer surface roughness can increase select osteoblast adhesion on carbon nanofiber compacts,[20] limited evidence on its cytocompatible properties currently exists, which leads to the decreased functions of astrocytes on carbon nanofiber materials.[18] This work improved greatly the hydrophilicity and/or biocompatibility of CNF by an acidic treatment process, which produced soluble CNF with a range of oxygen-containing groups on the surface of CNF without degradation of the structural integrity of its backbone.[21] These groups are in favor of adhesion and immobilization of cells.[22] Moreover, they can interact with the reactive amino and hydroxyl functional groups of CS to form a soluble CNF-doped CS colloidal solution. By combining the biocompatibility and good adhesion[23] of chitosan, the electrodeposited conductive architecture showed high compatibility for cells adhesion. The adhesion of K562 cells as a model on the architecture changed the electron-transfer impedance of the electrochemical probe, thus offering an opportunity for construction of an impedance cell sensor. Here, the CNF can act as an electron conductor for improving electrochemical cytosensing. The electrodeposited CS hydrogel could tightly attach to the electrode and retain its natural properties.[24]

Although the impedance sensors for cells have been developed,[25–27] their sensitivities are limited and the preparations also need to be simplified. An impedance sensor for *Escherichia coli* O157:H7, prepared by immobilizing anti-*E. coli* antibodies on an indium-tin oxide interdigitated array, showed a linear calibration in the concentration range from 4.36×10^5 to 4.36×10^8 cfu mL^{-1} and a detection limit of 10^6 cfu mL^{-1}.[25] Based on the immobilization of antibodies using an epoxysilane monolayer for chemical anchoring of antibodies and an enzymatic amplification process with alkaline phosphatase to label the anti-*E. coli* antibody, another impedance sensor for this cell showed a linear range from 6×10^4 and 6×10^7 cells mL^{-1} with a detection limit of 6×10^3 cells mL^{-1}.[26] These linear ranges were comparable with other label-free immunosensors for detection of pathogenic bacteria using different transducer techniques.[28–30] In this work the presence of CNF facilitated the electron transfer of adhered K562 cells, leading to sensitive voltammetric response of the K562. The detection limit of 1×10^3 cells mL^{-1} and wide linear range for detection of cell concentration showed higher sensitivity and better performance of the proposed impendence sensor due to the improved surface area of the CNF/CS. Furthermore, the preparation of this cell sensor was simple, convenient, and low-cost, suggesting a potential application of CNF in electrochemical cytosensing and related areas.

(19) Price, R. L.; Waid, M. C.; Haberstroh, K. M.; Webster, T. J. *Biomaterials* **2003**, *24*, 1877−1887.
(20) Price, R. L.; Ellison, K.; Haberstroh, K. M.; Webster, T. J. *J. Biomed. Mater. Res. A* **2004**, *70A*, 129−138.
(21) Maldonado, S.; Stevenson, K. J. *J. Phys. Chem. B* **2004**, *108*, 11375−11383.
(22) Kaji, H.; Kanada, M.; Oyamatsu, D.; Matsue, T.; Nishizawa, M. *Langmuir* **2004**, *20*, 16−19.
(23) Benesch, J.; Tengvall, P. *Biomaterials* **2002**, *23*, 2561−2568.
(24) Fernandes, R.; Wu, L. Q.; Chen, T.; Yi, H.; Rubloff, G. W.; Ghodssi, R.; Bentley, W. E.; Payne, G. F. *Langmuir* **2003**, *19*, 4058−4062.
(25) Yang, L.; Li, Y.; Erf, G. F. *Anal. Chem.* **2004**, *76*, 1107−1113.
(26) Ruan, C.; Yang, L.; Li, Y. *Anal. Chem.* **2002**, *74*, 4814−4820.
(27) Yang, L.; Li, Y.; Griffis, C. L.; Johnson, M. G. *Biosens. Bioelectron.* **2004**, *19*, 1139−1147.
(28) Park, I.; Kim, W.; Kim, N. *Biosens. Bioelectron.* **2000**, *15*, 167−172.
(29) Koubova, V.; Brynda, E.; Karasova, L.; Skvor, J.; Homola, J.; Dostalek, J.; Tobiska, P.; Rosicky, J. *Sens. Actuators, B* **2001**, *74*, 100−105.
(30) Fratamico, P. M.; Strobaugh, T. P.; Medina, M. B.; Gehring, A. G. *Biotechnol. Tech.* **1998**, *12*, 571−576.

EXPERIMENTAL SECTION

Materials and Reagents. CNF was a gift from WPI (Sarasota, FL). CS was obtained from Aldrich (Milwaukee, WI). All other chemicals were of analytical grade and used without further purification. Phosphate-buffered saline (PBS, pH 7.4) contained 136.7 mmol L^{-1} NaCl, 2.7 mmol L^{-1} KCl, 0.087 mol L^{-1} Na_2HPO_4, and 0.014 mol L^{-1} KH_2PO_4. All solutions were prepared with doubly distilled water.

CS solution (1%, wt %) was prepared by ultrasonically dissolving CS flakes in 1% acetic acid. After undissolved material was filtered, the pH was adjusted to about 5.0 using 1.0 mol L^{-1} NaOH. The solution was stored in a refrigerator (4 °C) before use.

CNF of certain mass was boiled in 30% nitric acid for 24 h to obtain carboxylic group-functionalized CNF.[13] After centrifugation from the mixture, the sediment was washed with doubly distilled water until the pH reached 7.0, dried under vacuum at 100 °C, and dispersed in above-mentioned CS solution to obtain soluble CNF-doped CS (CNF−CS) colloidal solution with aid of ultrasonic agitation for 6 h. As a control, the untreated CNF with the same content was dispersed in the CS solution.

Electrochemical Measurements and Preparation of CNF−CS Film. All electrochemical measurements were performed on a CHI 660 electrochemical analyzer (Co. CHI, TX) with a conventional three-electrode system comprised of platinum wire as auxiliary electrode, saturated calomel electrode (SCE) as reference, and modified glassy carbon electrode (GCE, diameter 3.0 mm) as working electrode at room temperature. Electrochemical impedance spectroscopy (EIS) was performed with an Autolab Electrochemical Analyzer (Eco Chemie, Netherlands) in 10 mM $K_3Fe(CN)_6/K_4Fe(CN)_6$ (1:1) mixture with 1.0 M KCl as supporting electrolyte, using an alternating current voltage of 5.0 mV, within the frequency range of 1−10^6 Hz.

The GCE was successively polished to a mirror finish using 0.3 and 0.05 μm alumina slurry (Beuhler, IL) followed by rinsing thoroughly with water. After successive sonication in 1:1 nitric acid, acetone, and doubly distilled water, the electrode was rinsed with doubly distilled water and allowed to dry at room temperature. Electrochemical deposition process was performed by dipping the GCE in a CNF−CS solution at −2.5 V for 300 s, unless otherwise noted, the contents of CS and soluble CNF were 1.0% and 0.5 mg mL^{-1}, respectively. The electrode was then removed from the solution and rinsed with water to obtain a CNF−CS nanocomposite film-modified electrode. For comparison, the CS-modified electrode was prepared in an analogous process. The formed films were aged in air for 6 h. The CNF film was formed by dropping 3.0 μL of 0.5 mg mL^{-1} treated CNF solution on the pretreated GCE and dried in a silica gel desiccator. All the modified electrodes were stored in air prior to use.

Cells Culture and Immobilization. The K562 cells were cultured in a flask in RPMI 1640 medium (GIBCO, Grand Island, NY) supplemented with 10% fetal bovine serum (Sigma, U.K.), penicillin (100 μg mL^{-1}), and streptomycin (100 μg mL^{-1}) in an incubator (5% CO_2, 37 °C). At the growth retardation stage (3 days), the cells reached a number of 1.0×10^7 cells mL^{-1}, which was determined using a Petroff−Hausser counter. They were

Scheme 1. Preparation of CNF−CS Film and Impendence Sensor for K562 Cells

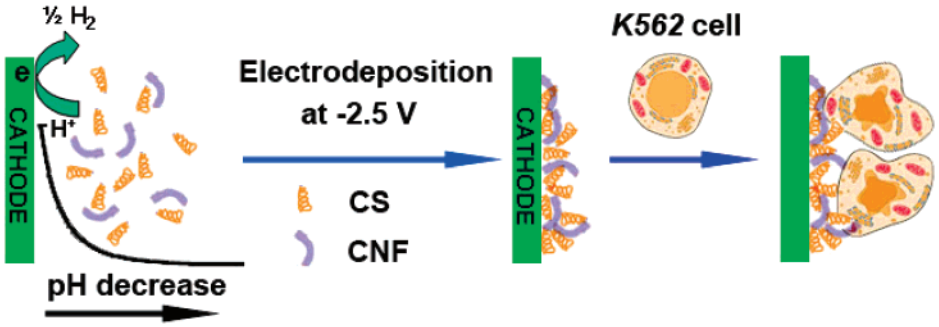

collected, separated from the medium by centrifugation at 1000 *g* for 10 min, and then washed twice with sterile PBS (pH 7.4). The sediments were resuspended in PBS to obtain cell suspension with the final concentration of cells equal to 5.0×10^7 cells mL^{-1}. The cell suspensions with various contents were prepared from this stock. After 2 μL of the cell suspension was dropped on the formed CNF−CS architecture and incubated at 37 °C for 2 h, the cells could be immobilized on the electrodes successfully.

Apparatus. Scanning electron microscopic (SEM) images of CNF and CNF−CS films formed on ITO slides were obtained on a LEO 1530 VP SEM (Germany). FT-IR spectra were recorded on a Nexus model 870 Fourier Transform IR Spectrophotometer (Thermo Electron. Corp., MA). Samples were thoroughly ground with exhaustively dried KBr. The solids of CS and CNF−CS were washed with doubly distilled water in order to remove NaCl that was formed in CS solutions during the pH adjustment. Thermogravimetry (TGA) was performed with a Pyres 1 TGA apparatus (PerkinElmer, MA) at a heating rate of 20 °C min^{-1} from room temperature to 800 °C under a nitrogen atmosphere. The static water contact angles were measured with a contact angle meter using droplets of deionized water at 25 °C. The readings were stabilized and taken at 120 s after dropping.

RESULTS AND DISCUSSION

Electrodeposition of CNF−CS Film. After the CNF was treated with nitric acid, it could disperse completely in the CS solution to form a clear black CNF−CS colloidal solution. This solution could preserve clearness for several months. However, the dispersion of untreated CNF in water or acidic solution was limited. It could also not disperse in the CS solution. The improvement of dispersion or solubility resulted from the acidic treatment process, in which a large number of oxygen-containing groups were formed on the surface of CNF.[13] These groups enhanced greatly the hydrophilicity of CNF and could interact with the reactive amino and hydroxyl functional groups of CS to form a monodisperse CNF−CS colloidal solution.

At the applied potential of −2.5 V the H^+ in CNF−CS colloidal solution could be reduced to H_2, resulting in gradually increased pH value at the electrode surface. As the solubility of CS is pH-dependent, when the pH was higher than the pK_a of CS (about 6.3), dissolved CS flocculated to form an insoluble hydrogel network due to the deprotonation of its amine groups (Scheme 1). As a result, CS hydrogel incorporated with CNF was electrodeposited on the cathode surface. Because of the generation of a CS gradient above the cathode surface more CS would diffuse to the cathode from the distance, and continuous electrochemical reduction of H^+ produced more insoluble hydrogel to be deposited onto the cathode surface. Finally, a CNF−CS architecture was formed on the electrode surface.

Characterization of CNF-CS Architecture. The SEM of CNF film prepared with the treated CNF displayed an enlaced three-dimensional incompact structure (Figure 1a). The diameter of the CNF was about 40 nm. The enlacement could be decreased in the electrodeposited CNF−CS architecture (Figure 1b), leading to a somewhat complanate surface. Such surface was favorable for cells loading and adhesion.

The FT-IR spectrum of CS displayed several peaks of the assigned saccharine structure around 1155, 1071, and 1029 cm^{-1} [31] and a strong acylamide characteristic peak at 1650 cm^{-1}, while the treated CNF showed the peaks of hydroxyl group at 3401 cm^{-1}, carboxyl group at 1726 cm^{-1}, and carboxylate group at 1584 and 1383 cm^{-1} (Figure 2). The existence of carboxylate groups might be attributed to the electroionization of the carboxyl groups.[32] These groups made the treated CNF easy to be dispersed in water and CS.[33] For CNF−CS powder, the peaks of these groups could also be observed, but the positions for both hydroxyl and carboxylate groups shifted in blue to 3424, 1593, and 1385 cm^{-1}, indicating their interaction with the reactive amino and hydroxyl functional groups of CS to form a hydrogen bond, which resulted in red shift of the peaks at 1155 and 1071 cm^{-1} for CS to 1141 and 1057 cm^{-1}, respectively.

The TGA curves of the solid powder samples of treated CNF, CS, and CNF−CS in a nitrogen atmosphere were shown in Figure 3. From room temperature to 600 °C the TGA curve of the CNF was somewhat planar, and the mass loss that occurred at temperatures higher than 600 °C (curve a) perhaps could be ascribed to the destruction of functional groups attached to CNFs.[34] This data indicated the good stability and high purity of CNF.

TGA of the CS sample (Figure 3A, curve b) showed that the thermal decomposition of CS took place in one step from 260 to 400 °C basically after the initial elimination of residual water (~20−100 °C), which was ascribed to the depolymerization and decomposition of glucosamine units of CS, similar to the result

(31) Wan, Y.; Wu, H.; Yu, A.; Wen, D. *Biomacromolecules* **2006**, *7*, 1362−1372.
(32) Luo, H.; Shi, Z.; Li. N.; Gu, Z.; Zhuang, Q. *Anal. Chem.* **2001**, *73*, 915−920.
(33) Jiang, K.; Eitan, A.; Schadler, L. S.; Ajayan, P. M.; Siegel, R. W. *Nano Lett.* **2003**, *3*, 275−277.
(34) Lian, Y.; Maeda, Y.; Wakahara, T.; Akasaka, T.; Kazaoui, S. *J. Phys. Chem. B* **2004**, *108*, 8848−8854.

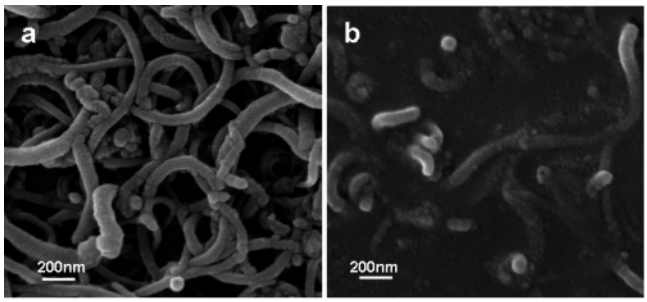

Figure 1. Scanning electron micrographs of (a) CNF and (b) CNF−CS films.

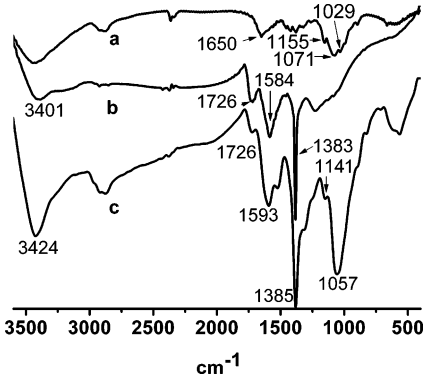

Figure 2. Infrared spectra of (a) CS, (b) soluble CNF, and (c) soluble CNF-doped CS powders.

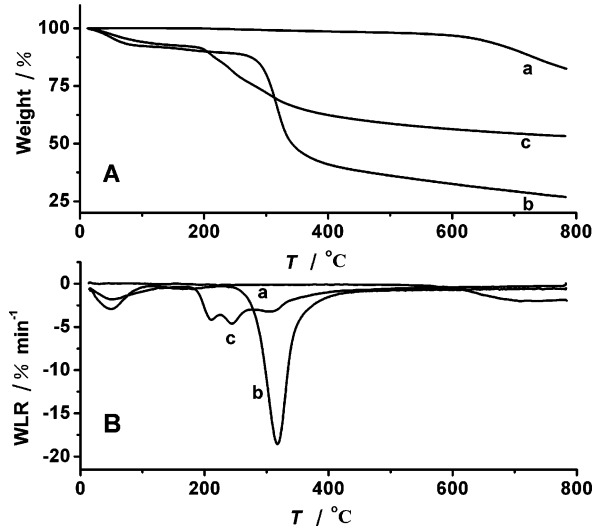

Figure 3. (A) TGA and (B) DTG traces for (a) soluble CNF, (b) CS, and (c) soluble CNF-doped CS powders. WRL: abbreviation of the weight loss rate.

reported previously.[35] The decomposition step yielded an obvious narrow peak, and the mass loss rate of CS reached a maximum value of 18.6% min^{-1} at 316 °C (Figure 3B, curve b). The mass of CS decreased slowly in the temperature range from 400 to 800 °C, which corresponded to the gradual carbonization of CS. However, the TGA of the CNF−CS composite sample showed a lower thermal decomposition temperature and lower mass loss than CS, and its DTG showed three small peaks at 209, 244, and 314 °C (Figure 3, curve c), indicating different states of CS presented in the composite sample, tightly adsorbed CS on CNF

(35) Zhang, M. G.; Smith, A.; Gorski, W. *Anal. Chem.* **2004**, *76*, 5045−5050.

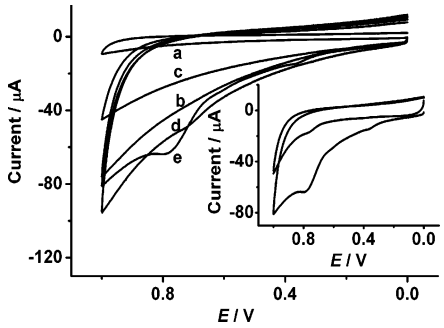

Figure 4. Cyclic voltammograms of (a) bare GCE, (b) CS/GCE, (c) CNF−CS/GCE, (d) K562 cells/CS/GCE, and (e) K562 cells/CNF−CS/GCE in pH 7.4 PBS. Inset: two continuous sweeps of sample in part e. Scan rate: 50 mV s^{-1}.

by hydrogen binding interaction, adsorbed CS by other molecular interactions such as van der Waals force, and free CS. The adsorption or molecular interactions made the thermal decomposition of CS take place at lower temperatures.[35]

The biocompatibility of a material for loading of biomolecules and preserving their bioactivity is positively related to its hydrophilicity,[36] which could be characterized with the contact angle measurement of the substrate. CNF−CS- and CS-deposited ITO glass slides gave the contact angles of 47.3 and 51 °C, respectively. CNF−CS gave a smaller contact angle than that of CS, demonstrating the excellent hydrophilicity of CNF−CS film. The hydrophilic CNF−CS film provided a favorable microenvironment for living cells, and thus longer life of the adhered cells on CNF−CS film than CS film was observed, indicating the better biocompatibility of CNF−CS toward the cells, which was highly advantageous to their adhesion, proliferation and retention of bioactivity.[22]

Voltammetric Behavior of K562 Cells Adhered on CNF−CS/GCE. Bare GCE, CNF−CS/GCE, and CS/GCE did not show any detectable cyclic voltammetric response in pH 7.4 PBS (Figure 4). The background current of the CNF−CS/GCE and CS/GCE was larger than that of the bare GCE due to the larger accessible surface area of the modified electrode. The presence of CNF in CS resulted in a decrease in the background current. After K562 cells were adhered on the CNF−CS/GCE, a well-defined peak and a small ill-defined anodic peak appeared at +0.823 and +0.360 V at 50 mV s^{-1}, respectively (Figure 4, curve e), while no peak was observed for the K562 cells adhered on CS/GCE (Figure 4, curve d), indicating the ability of CNF to promote electron-transfer reactions between electroactive centers of cells and the electrode. The anodic peak at +0.823 V could be ascribed to the oxidation of guanine within the cytoplasm of the living cells, which was able to cross the cell membrane rapidly during the electrochemical process,[37] and the another peak was caused by the oxidation of other electroactive components within the interior of cells because of the penetration of CNF into the drape of cells. These results indicated that the cells were successfully adhered on the CNF−CS film-modified electrode surface. Both oxidation peaks did not show any corresponding reduction signal in the inverse scan, and they dropped dramatically in the second scan (inset in Figure 4), which were characteristic of an irreversible electrode process.

(36) Zhu, A. P.; Zhang, M.; Wu, J.; Shen, J. *Biomaterials* **2002**, *23*, 4657−4665.
(37) Chen, J.; Du, D.; Yan, F.; Ju, H. X.; Lian, H. Z. *Chem. Eur. J.* **2005**, *11*, 1467−1472.

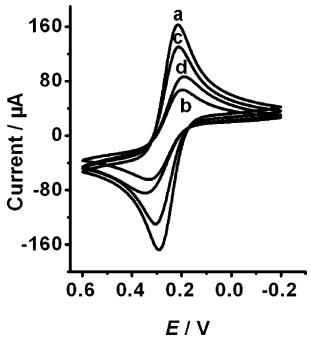

Figure 5. Cyclic voltammograms of 10 mM $[Fe(CN)_6]^{3-}$ in 1.0 M KCl at (a) bare GCE, (b) CS/GCE, (c) CNF−CS/GCE, and (d) K562 cells/CNF−CS/GCE prepared with 1×10^5 cells mL^{-1} K562 cells at 50 mV s^{-1}.

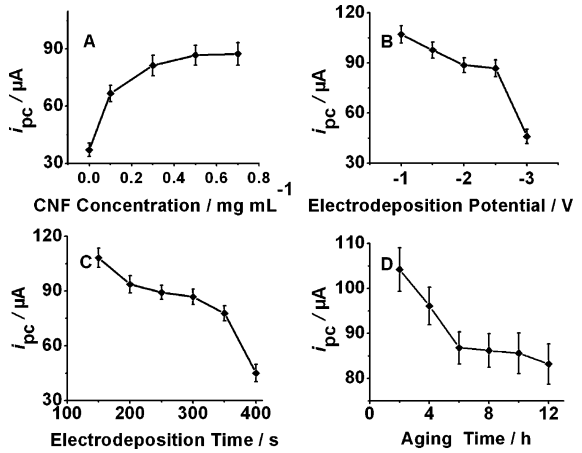

Figure 6. Effects of CNF concentration in soluble CNF-doped CS colloidal solution (A), electrodeposition potential (B), electrodeposition time (C), and aging time of CNF−CS film (D) on peak current of 10 mM $[Fe(CN)_6]^{3-}$ in 1.0 M KCl at the electrode as the same as Figure 5d. Scan rate: 50 mV s^{-1}.

Optimization of Electrodeposition Conditions of CNF−CS Film for Cytosensing. The sensitivity of a cell sensor based on the impedance measurement depends on the response of a redox probe at the sensor. Here the ferricyanide/ferrocyanide system was used as the redox probe for the impedance measurement. The cyclic voltammograms of ferricyanide at different electrodes were shown in Figure 5. With the formation of CS film at GCE, the peak currents decreased greatly, while the incorporation of CNF in the CS film resulted in great increases of the redox peaks in comparison with those at CS/GCE. Similarly, the peak currents at K562 cells/CNF−CS/GCE were also larger than those at K562 cells/CS/GCE. However, the peak potentials or their separation showed very slight change. Thus, CNF did not change the electron-transfer kinetics of ferricyanide/ferrocyanide; the increasing response was due to the improved surface area of the CNF/CS.

At the K562 cells/CNF−CS/GCE, the electrochemical signal of this probe was related to the preparation process of the CNF−CS film. Figure 6 shows the dependence of the reduction peak current of ferricyanide under different electrodeposition conditions, containing CNF concentrations in the CNF−CS solution, electrodeposition potential and time, and aging time. With the increasing concentration of CNF, the reduction peak current increased and approached a constant value (Figure 6a). Considering the fact that excessive CNF in film was adverse to the adhesion of cells, a concentration of 0.5 mg mL^{-1} was chosen, after which the increment of the peak current was very small.

The electrodeposition potential and time controlled the film thickness, which affected both the adhesion of cells on the formed CNF−CS film and the electron transfer of electroactive probe. At a more negative electrodeposition potential, the reduction of H^+ and the increase of pH value at the electrode surface were faster, resulting in quicker formation of an insoluble CNF incorporated hydrogel network. At the same electrodeposition time thicker CNF−CS film was formed. Thus the response of ferricyanide decreased slowly (Figure 6b). When the potential was more negative than −2.5 V, the overly rapid electrodeposition of CS allowed less CNF to be incorporated into the film; thus, the response of ferricyanide dropped dramatically. At the same time a coarse and uneven CNF−CS film was formed at −3.0 V, which was instable and unfavorable to the adhesion of cells. Considering the need for formation of CNF−CS film, −2.5 V was used for its electrodeposition, at which the electrodeposition time was a decisive factor for controlling the film thickness. As shown in Figure 6c, with the increasing electrodeposition time the response of ferricyanide decreased slowly and then dropped dramatically at an electrodeposition time of 300 s. Comparatively, the electrodeposition time of 300 s was suitable.

For cells adhesion, the aging of film was also an important step. With an increasing aging time the response of ferricyanide decreased and approached a stable value at 6 h (Figure 6d), which was selected as an optimal aging time for preparation of the cell sensor. Under optimized conditions, the obtained CNF−CS film was stable enough for the adhesion and detection of cells in a neutral solution. Although a dip-coating method with the same amounts of CNF and CS and even longer aging time could also form a film of CNF−CS composite on the electrode surface, it usually desquamated from the electrode surface upon the adhesion of cells.

Impedance Sensor for K562 Cells. The impedance measurements rely on the observation that living cells have excellent insulating properties at low frequencies and dielectric features at high frequencies. The membranes of natural biological cells (thickness 5−10 nm) show the capacitance of 0.5−1.3 μF cm^{-2} and the resistance of 10^2−10^5 Ω.[25] Thus, EIS has been used to monitor the adhesion of macrophages,[38] endothelial cells,[39] fibroblasts,[40] and bacterial cells[26,25] on modified electrodes. When K562 cells were adhered onto the CNF−CS film, the modified electrode showed an increased charge-transfer impedance (R_{et}) (Figure 7).

The EIS of $[Fe(CN)_6]^{3-}/[Fe(CN)_6]^{4-}$ probe at different modified electrodes showed different R_{et} values (Figure 7), similar to the change in cyclic voltammetric responses of $[Fe(CN)_6]^{3-}$ (Figure 5). At bare GCE the R_{et} value of 69 Ω was the lowest. Upon the formation of CS film, the R_{et} increased greatly to 1186 Ω, and the presence of CNF decreased the charge-transfer impedance from 1186 Ω to 390 Ω because of its favorably high

(38) Mitra, P.; Keese, C. R.; Lawrence, D. A.; Giaever, I. *Biotechniques* **1990**, *11*, 504−510.
(39) Xiao, C.; Lachance, B.; Sunahara, G.; Luong, J. H. T. *Anal. Chem.* **2002**, *74*, 1333−1339.
(40) Luong, J. H. T.; Habibi-Razaei, M.; Meghrous, J.; Xiao, C.; Male, K. B.; Kamen, A. *Anal. Chem.* **2001**, *73*, 1844−1848.

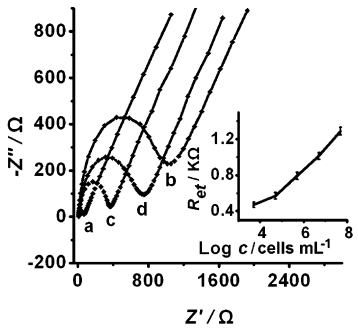

Figure 7. Nyquist diagrams of Faradaic impedance spectra recorded in a frequency range of $1-10^6$ Hz for $[Fe(CN)_6]^{3-}/[Fe(CN)_6]^{4-}$ (10 mM, 1:1) in 1.0 M KCl at the electrodes, using the same conditions as in Figure 6. Inset: Calibration curve of the impedance sensor for K562 cells.

electrical transport properties. When cells were attached to the CNF−CS/GCE, a barrier would hamper the redox probe close to the electrode surface and increase the charge-transfer impedance (Figure 7, curves c and d). The increasing impedence depended on the surface coverage of the cells, which was proportional to the concentration of the cells used in the adhesion process. Thus, with the increasing concentration of K562 cells the R_{et} value increased, showing a semilogarithmic dependence of the R_{et} value on the concentration of K562 cells used for cells adhesion, as shown in the inset of Figure 7. Thus, the CNF−CS/GCE could be used for detection of K562 cell concentration.

The EIS measurement was more sensitive than the cyclic voltammetric measurement for sensing the change in cell concentration. When 1×10^5 cells mL^{-1} K562 cells were adhered on the CNF−CS/GCE, the increase in R_{et} value was 104%, whereas the decrease in the peak current was only 34%. The R_{et} value was proportional to the logarithm of K562 cell concentration in the range of 5×10^3 to 5.0×10^7 cells mL^{-1} with a limit of detection of 1×10^3 cells mL^{-1}, at which the increase of R_{et} value was 3 times the standard deviation of R_{et} detected at the CNF−CS/GCE. The cell sensor showed higher sensitivity than those with the limits of detection of 10^6 cfu mL^{-1} [25] and 6×10^3 cells mL^{-1} [26] for *Escherichia coli* O157:H7.

The reproducibility of the impedance sensor for K562 cells was estimated from the slopes of six calibration plots obtained with freshly prepared CNF−CS-modified electrodes. The relative standard deviation of the slopes was 4.2%. At the cell concentrations of 5.0×10^6 and 5.0×10^7 cells mL^{-1}, the sensor showed the relative standard deviation of 4.1% and 3.4% examined for six determinations, respectively, showing good precision.

CONCLUSIONS

This work uses nitric acid-treated CNF as an electron conductor to prepare a sensitive impedance sensor by a controllable electrodeposition process in soluble CNF-doped CS colloidal solution. The FT-IR and thermogravimetric analyses indicate that the interactions between the oxygen-containing groups of treated CNF and the reactive amino and hydroxyl functional groups of CS result in the formation of the colloidal solution. By combining the biocompatibility and good adhesion of chitosan, the electrodeposited conductive architecture is suitable for the adhesion and immobilization of K562 cells, producing a sensitive impedance cell sensor. The proposed sensor for K562 cells shows good fabrication reproducibility and detection precision. This research could open new avenues in CNF applications for cytosensing and provide a convenient platform to modify for clinical testing, drug screening, and discovery in the future. Further work is underway in our labs.

ACKNOWLEDGMENT

We gratefully acknowledge the National Science Funds for Distinguished Young Scholars (20325518) and Creative Research Groups (20521503), the Key Program (20535010) from the National Natural Science Foundation of China, and the Science Foundation of Jiangsu (BS2006006, BS2006074) for financial support of this research.

Received for review December 12, 2006. Accepted April 8, 2007.

AC062344Z